Geomechanics and Engineering, *Vol. 8, No. 3 (2015) 305-321*
DOI: http://dx.doi.org/10.12989/gae.2015.8.3.305

A new hyperbolic shear deformation plate theory for static analysis of FGM plate based on neutral surface position

M. Merazi [1], L. Hadji [*1,2], T.H. Daouadji [1,2],
Abdelouahed Tounsi [1] and E.A. Adda Bedia [1]

[1] *Material and Hydrology Laboratory, University of Sidi Bel Abbes, Faculty of Technology, Civil Engineering Department, Algeria*
[2] *Université Ibn Khaldoun, BP 78 Zaaroura, 14000 Tiaret, Algérie*

(*Received May 25, 2014, Revised November 11, 2014, Accepted November 17, 2014*)

Abstract. In this paper, a new hyperbolic shear deformation plate theory based on neutral surface position is developed for the static analysis of functionally graded plates (FGPs). The theory accounts for hyperbolic distribution of the transverse shear strains and satisfies the zero traction boundary conditions on the surfaces of the beam without using shear correction factors. The neutral surface position for a functionally graded plate which its material properties vary in the thickness direction is determined. The mechanical properties of the plate are assumed to vary continuously in the thickness direction by a simple power-law distribution in terms of the volume fractions of the constituents. Based on the present new hyperbolic shear deformation plate theory and the neutral surface concept, the governing equations of equilibrium are derived from the principle of virtual displacements. Numerical illustrations concern flexural behavior of FG plates with Metal-Ceramic composition. Parametric studies are performed for varying ceramic volume fraction, volume fraction profiles, aspect ratios and length to thickness ratios. The accuracy of the present solutions is verified by comparing the obtained results with the existing solutions.

Keywords: mechanical properties; functionally graded material; neutral surface position; shear deformation; volume fraction

1. Introduction

Functionally graded materials (FGMs) are a class of composites that have continuous variation of material properties from one surface to another and thus eliminate the stress concentration found in laminated composites. A typical FGM is made from a mixture of two material phases, for example, a ceramic and a metal. The reason for the increasing use of FGMs in a variety of aerospace, automotive, civil, and mechanical engineering structures is that their material properties can be tailored to different applications and working environments (Reddy 2000, El Meiche *et al.* 2011, Talha and Singh 2011, Jha *et al.* 2011, Ebrahimi 2013, Houari *et al* 2013, Attia *et al.* 2015, Bachir Bouiadjra *et al.* 2013, Tounsi *et al.* 2013, Saidi *et al.* 2013, Bessaim *et al.* 2013, Chakraverty and Pradhan 2014, Hebali *et al.* 2014, Khalfi *et al.* 2014, Belabed *et al.* 2014, Swaminathan and Naveenkumar 2014, Zidi *et al.* 2014, Hamidi *et al.* 2015). Now, FGMs are

*Corresponding author, Ph.D., E-mail: had_laz@yahoo.fr

http://www.techno-press.org/?journal=gae&subpage=7 ISSN: 2005-307X (Print), 2092-6219 (Online)

developed for general use as structural components in extremely high temperature environments. Several studies have been performed to analyze the mechanical or the thermal or the thermomechanical responses of FG plates and shells. Reddy (2000) has analyzed the static behavior of functionally graded rectangular plates based on his third-order shear deformation plate theory. Jha *et al* (2011) presented static stress analysis response of FG plates based on higher order shear and normal deformation theory. Taj *et al*. (2013) conducted static analysis of FG plates using higher order shear deformation theory. Transverse shear stresses are represented as quadratic through the thickness and hence it requires no shear correction factor. Benachour *et al*. (2011) studied the free vibration of FG plates with an arbitrary gradient. A higher order shear deformation model for FG has been examined by Dharan *et al.* (2010) using zeroth order shear deformation theory (ZSDT).

Recently, Tounsi and his co-workers (Hadji *et al*. 2011, Houari *et al*. 2011, El Meiche *et al*. 2011, Bourada *et al*. 2012, Bachir Bouiadjra *et al*. 2012, Fekrar *et al*. 2012, Fahsi *et al*. 2012, Bouderba *et al*. 2013, Kettaf *et al*. 2013, Klouche Djedid *et al*. 2014, Nedri *et al*. 2014, Ait Amar Meziane *et al*. 2014, Draiche *et al*. 2014, Sadoune *et al*. 2014, Ait Yahia *et al*. 2015, Belkorissat *et al*. 2015) developed new shear deformation plates theories involving only four unknown functions.

In the present article, a new hyperbolic shear deformation plate theory based on neutral surface position is developed for the static analysis of functionally graded plates. This theory has number of advantages over the CLPT and FSDPT. It is possible to take into account the higher order effects and yet keep the complexity to a considerably lower level. In the present theory the governing differential equation is of fourth order and in these only lateral deflection, plate physical properties and lateral loading are being used. The governing equations of equilibrium are obtained from the principle of virtual displacements and Navier solutions for flexure of FG simply supported plates are presented. The accuracy and effectiveness of the present theory are established through numerical examples. Numerical results are presented for Ceramic – Metal functionally graded plates.

2. Theoretical formulations

2.1 Physical neutral surface

Functionally graded materials are a special kind of composites in which their material properties vary smoothly and continuously due to gradually varying the volume fraction of the constituent materials along certain dimension (usually in the thickness direction). In this study, the FG plate is made from a mixture of ceramic and metal and the properties are assumed to vary through the thickness of the plate. Due to asymmetry of material properties of FG plates with respect to middle plane, the stretching and bending equations are coupled. But, if the origin of the coordinate system is suitably selected in the thickness direction of the FG plate so as to be the neutral surface, the properties of the FG plate being symmetric with respect to it. To specify the position of neutral surface of FG plates, two different planes are considered for the measurement of z, namely, z_{ms} and z_{ns} measured from the middle surface and the neutral surface of the plate, respectively, as depicted in Fig. 1.

The volume-fraction of ceramic V_C is expressed based on z_{ms} and z_{ns} coordinates as

$$V_C = \left(\frac{z_{ms}}{h} + \frac{1}{2}\right)^n = \left(\frac{z_{ns} + C}{h} + \frac{1}{2}\right)^n \tag{1}$$

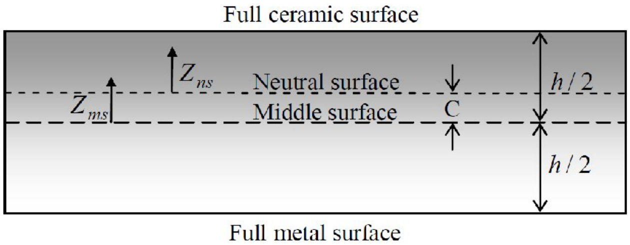

Fig. 1 The position of middle surface and neutral surface for a functionally graded plate

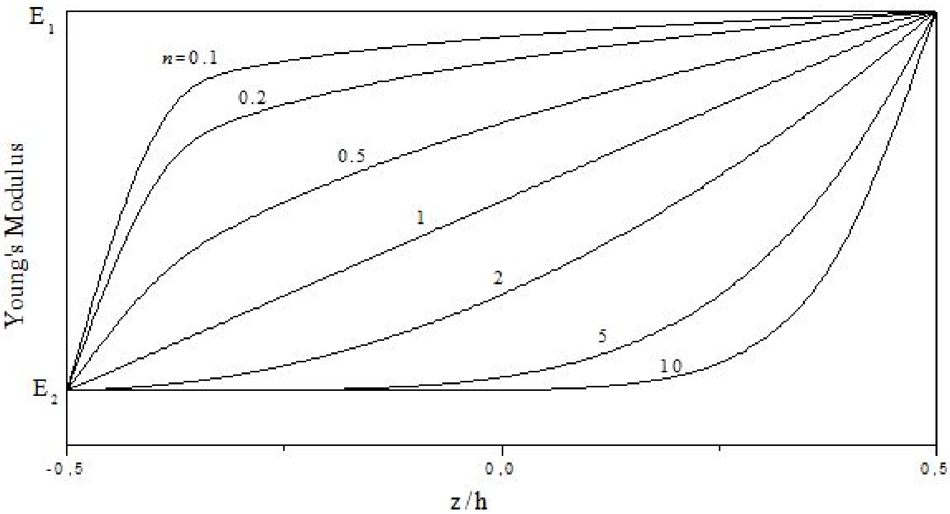

Fig. 2 Variation of Young's modulus in a *P*-FGM plate

where n is the power law index which takes the value greater or equal to zero and C is the distance of neutral surface from the mid-surface. Material non-homogeneous properties of a functionally graded material plate may be obtained by means of the Voigt rule of mixture (Suresh and Mortensen 1998). Thus, using Eq. (1), the material non-homogeneous properties of FG plate P, as a function of thickness coordinate, become

$$P(z) = P_M + P_{CM}\left(\frac{z_{ns} + C}{h} + \frac{1}{2}\right)^n, \quad P_{CM} = P_C - P_M \tag{2}$$

where P_M and P_C are the corresponding properties of the metal and ceramic, respectively. In the present work, we assume that the elasticity modules E and the mass density ρ are described by Eq. (2), while Poisson's ratio v, is considered to be constant across the thickness (Benachour *et al.* 2011, Larbi Chaht *et al.* 2014).

The variation of Young's modulus in the thickness direction of the *P*-FGM plate is depicted in Fig. 2, which shows that the Young's modulus changes rapidly near the lowest surface for $n \succ 1$ and increases quickly near the top surface for $n \prec 1$.

The position of the neutral surface of the FG plate is determined to satisfy the first moment with respect to Young's modulus being zero as follows (Bouremana *et al*. 2013, Ould Larbi *et al*. 2013, Fekrar *et al*. 2014, Bousahla *et al*. 2014)

$$\int_{-h/2}^{h/2} E(z_{ms})(z_{ms} - C)dz_{ms} = 0 \tag{3}$$

The position of neutral surface can be obtained as

$$C = \frac{\int_{-h/2}^{h/2} E(z_{ms}) z_{ms} dz_{ms}}{\int_{-h/2}^{h/2} E(z_{ms}) dz_{ms}} \tag{4}$$

From Eq. (6), it can be seen that the parameter C is zero for homogeneous isotropic plate as expected.

2.2 Basic assumptions

Consider a plate of total thickness h and composed of functionally graded material through the thickness (Fig. 3). It is assumed that the material is isotropic and grading is assumed to be only through the thickness.

The assumptions of the present theory are as follows:

(i) The origin of the Cartesian coordinate system is taken at the neutral surface of the FG plate.
(ii) The displacements are small in comparison with the height of the plate and, therefore, strains involved are infinitesimal.
(iii) The transverse displacement w includes two components of bending w_b, and shear w_s. These components are functions of coordinates x, y only.

$$w(x, z_{ns}, t) = w_b(x,t) + w_s(x,t) \tag{5}$$

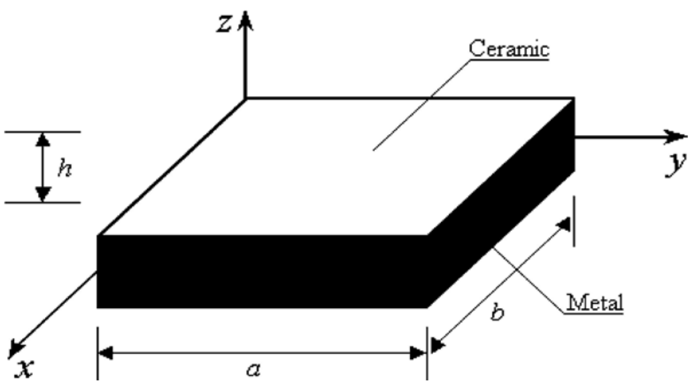

Fig. 3 Geometry of rectangular plate composed of FGM

(iv) The transverse normal stress σ_z is negligible in comparison with in-plane stresses σ_x and σ_y.

(v) The axial displacement u in x-direction, consists of extension, bending, and shear components.

$$u = u_0 + u_b + u_s, \quad v = v_0 + v_b + v_s \tag{6}$$

(vi) The bending component u_b and v_b are assumed to be similar to the displacements given by the classical plate theory. Therefore, the expression for u_b and v_b can be given as

$$u_b = -z_{ns}\frac{\partial w_b}{\partial x}, \quad v_b = -z_{ns}\frac{\partial w_b}{\partial y} \tag{7}$$

(vii) The shear components u_s and v_s gives rise, in conjunction with w_s, to the hyperbolic variation of shear strains γ_{xz}, γ_{yz} and hence to shear stresses τ_{xz}, τ_{yz} through the thickness of the plate in such a way that shear stresses τ_{xz}, τ_{yz} are zero at the top and bottom faces of the plate. Consequently, the expression for u_s and v_s can be given as

$$u_s = -f(z_{ns})\frac{\partial w_s}{\partial x}, \quad v_s = -f(z_{ns})\frac{\partial w_s}{\partial y} \tag{8}$$

where

$$f(z_{ns}) = \left(z_{ns} + C\right)\left[1 + \frac{3\pi}{2}\sec h^2\left(\frac{1}{2}\right)\right] - \frac{3\pi}{2}h\tanh\left(\frac{z_{ns}+C}{h}\right) \tag{9}$$

2.3 Kinematics and constitutive equations

Based on the assumptions made in the preceding section, the displacement field can be obtained using Eqs. (5)-(9) as

$$\begin{aligned} u(x,y,z_{ns}) &= u_0(x,t) - z_{ns}\frac{\partial w_b}{\partial x} - f(z_{ns})\frac{\partial w_s}{\partial x} \\ v(x,y,z_{ns}) &= v_0(x,t) - z_{ns}\frac{\partial w_b}{\partial y} - f(z_{ns})\frac{\partial w_s}{\partial y} \\ w(x,y,z_{ns}) &= w_b(x,y) + w_s(x,y) \end{aligned} \tag{10}$$

The strains associated with the displacements in Eq. (10) are

$$\begin{aligned} \varepsilon_x &= \varepsilon_x^0 + z_{ns}\,k_x^b + f(z_{ns})\,k_x^s \\ \varepsilon_y &= \varepsilon_y^0 + z_{ns}\,k_y^b + f(z_{ns})\,k_y^s \\ \gamma_{yz} &= g(z_{ns})\,\gamma_{yz}^s \\ \gamma_{xz} &= g(z_{ns})\,\gamma_{xz}^s \\ \varepsilon_z &= 0 \end{aligned} \tag{11}$$

where

$$\varepsilon_x^0 = \frac{\partial u_0}{\partial x}, \quad k_x^b = -\frac{\partial^2 w_b}{\partial x^2}, \quad k_x^s = -\frac{\partial^2 w_s}{\partial x^2},$$

$$\varepsilon_y^0 = \frac{\partial v_0}{\partial x}, \quad k_y^b = -\frac{\partial^2 w_b}{\partial y^2}, \quad k_y^s = -\frac{\partial^2 w_s}{\partial y^2}, \tag{12}$$

$$\gamma_{yz}^s = \frac{\partial w_s}{\partial x}, \quad \gamma_{xz}^s = \frac{\partial w_s}{\partial x}, \quad g(z_{ns}) = 1 - f'(z_{ns}) \quad \text{and} \quad f'(z_{ns}) = \frac{df(z_{ns})}{dz_{ns}}$$

For elastic and isotropic FGMs, the constitutive relations can be written as:

$$\begin{Bmatrix} \sigma_x \\ \sigma_y \\ \tau_{yz} \\ \tau_{xz} \\ \tau_{xy} \end{Bmatrix} = \begin{bmatrix} Q_{11} & Q_{12} & 0 & 0 & 0 \\ Q_{12} & Q_{22} & 0 & 0 & 0 \\ 0 & 0 & Q_{44} & 0 & 0 \\ 0 & 0 & 0 & Q_{55} & 0 \\ 0 & 0 & 0 & 0 & Q_{66} \end{bmatrix} \begin{Bmatrix} \varepsilon_x \\ \varepsilon_y \\ \gamma_{yz} \\ \gamma_{xz} \\ \gamma_{xy} \end{Bmatrix} \tag{13}$$

where

$$Q_{11}(z_{ns}) = \frac{E(z_{ns})}{(1-\nu^2)}, \tag{14a}$$

$$Q_{12}(z_{ns}) = \nu Q_{11}(z_{ns}) \tag{14b}$$

$$Q_{44}(z_{ns}) = Q_{55}(z_{ns}) = Q_{66}(z_{ns}) = \frac{E(z_{ns})}{2(1+\nu)} \tag{14c}$$

2.4 Governing equations

The governing equations of equilibrium can be derived by using the principle of virtual displacements. The principle of virtual work in the present case yields

$$\int_{-h/2-C}^{h/2-C} \int_{\Omega} [\sigma_x \delta\varepsilon_x + \sigma_y \delta\varepsilon_y + \tau_{xy}\delta\gamma_{xy} + \tau_{yz}\delta\gamma_{yz} + \tau_{xz}\delta\gamma_{xz}]\, d\Omega dz - \int_{\Omega} q\delta w d\Omega = 0, \tag{15}$$

Where Ω is the top surface and q is the applied transverse load.

Substituting Eqs. (11) and (13) into Eq. (15) and integrating through the thickness of the plate, Eq. (15) can be rewritten as

$$\int_{\Omega} \begin{bmatrix} N_x \delta\varepsilon_x^0 + N_y \delta\varepsilon_y^0 + N_{xy}\delta\gamma_{xy}^0 + M_x^b \delta k_x^b + M_y^b \delta k_y^b + M_{xy}^b \delta k_{xy}^b \\ + M_x^s \delta k_x^s + M_y^s \delta k_y^s + M_{xy}^s \delta k_{xy}^s + S_{yz}^s \delta\gamma_{yz}^s + S_{xz}^s \delta\gamma_{xz}^s \end{bmatrix} d\Omega - \int_{\Omega} q\delta w d\Omega = 0, \tag{16}$$

where

$$\begin{Bmatrix} N_x, & N_y, & N_{xy} \\ M_x^b, & M_y^b, & M_{xy}^b \\ M_x^s, & M_y^s, & M_{xy}^s \end{Bmatrix} = \int_{-h/2-C}^{h/2-C} \left(\sigma_x, \sigma_y, \tau_{xy}\right) \begin{Bmatrix} 1 \\ z \\ f(z_{ns}) \end{Bmatrix} dz_{ns} \tag{17a}$$

$$\left(S_{xz}^s, S_{yz}^s\right) = \int_{-h/2-c}^{h/2-c} (\tau_{xz}, \tau_{yz}) g(z_{ns}) dz_{ns} \tag{17b}$$

The governing equations of equilibrium can be derived from Eq. (16) by integrating the displacement gradients by parts and setting the coefficients zero δu_0, δv_0, δw_b, and δw_s separately. Thus one can obtain the equilibrium equations associated with the present new hyperbolic shear deformation theory

$$\begin{aligned} &\delta u_0: \ \frac{\partial N_x}{\partial x} + \frac{\partial N_y}{\partial y} = 0 \\ &\delta v_0: \ \frac{\partial N_{xy}}{\partial x} + \frac{\partial N_y}{\partial y} = 0 \\ &\delta w_b: \ \frac{\partial^2 M_x^b}{dx^2} + 2\frac{\partial^2 M_{xy}^b}{\partial x^2 \partial y^2} + \frac{\partial^2 M_y^b}{dy^2} + q = 0 \\ &\delta w_s: \ \frac{\partial^2 M_x^s}{dx^2} + 2\frac{\partial^2 M_{xy}^s}{\partial x^2 \partial y^2} + \frac{\partial^2 M_y^s}{dy^2} + \frac{\partial S_{xz}^s}{\partial x} + \frac{\partial S_{yz}^s}{\partial y} + q = 0 \end{aligned} \tag{18}$$

Using Eq. (13) in Eq. (17), the stress resultants of a the plate can be related to the total strains by

$$\begin{Bmatrix} N \\ M^b \\ M^s \end{Bmatrix} = \begin{bmatrix} A & 0 & B^s \\ 0 & D & D^s \\ B^s & D^s & H^s \end{bmatrix} \begin{Bmatrix} \varepsilon \\ k^b \\ k^s \end{Bmatrix}, \quad \begin{Bmatrix} S_{yz}^s \\ S_{xz}^s \end{Bmatrix} = \begin{bmatrix} A_{44}^s & 0 \\ 0 & A_{55}^s \end{bmatrix} \begin{Bmatrix} \gamma_{yz}^s \\ \gamma_{xz}^s \end{Bmatrix} \tag{19}$$

where

$$N = \{N_x, N_y, N_{xy}\}^t, \quad M^b = \{M_x^b, M_y^b, M_{xy}^b\}^t, \quad M^s = \left\{M_x^s, M_y^s, M_{xy}^s\right\}^t \tag{20a}$$

$$\varepsilon = \{\varepsilon_x^0, \varepsilon_y^0, \gamma_{xy}^0\}, \quad k^b = \{k_x^b, k_y^b, k_{xy}^b\}, \quad k^s = \{k_x^s, k_y^s, k_{xy}^s\} \tag{20b}$$

$$A = \begin{bmatrix} A_{11} & A_{12} & 0 \\ A_{12} & A_{22} & 0 \\ 0 & 0 & A_{66} \end{bmatrix}, \quad D = \begin{bmatrix} D_{11} & D_{12} & 0 \\ D_{12} & D_{22} & 0 \\ 0 & 0 & D_{66} \end{bmatrix}, \quad B^s = \begin{bmatrix} B_{11}^s & B_{12}^s & 0 \\ B_{12}^s & B_{22}^s & 0 \\ 0 & 0 & B_{66}^s \end{bmatrix} \tag{20c}$$

$$D^s = \begin{bmatrix} D_{11}^s & D_{12}^s & 0 \\ D_{12}^s & D_{22}^s & 0 \\ 0 & 0 & D_{66}^s \end{bmatrix}, \quad H^s = \begin{bmatrix} H_{11}^s & H_{12}^s & 0 \\ H_{12}^s & H_{22}^s & 0 \\ 0 & 0 & H_{66}^s \end{bmatrix} \tag{20d}$$

where A_{ij}, D_{ij}, etc., are the plate stiffness, defined by

$$\begin{Bmatrix} A_{11} & D_{11} & B_{11}^s & D_{11}^s & H_{11}^s \\ A_{12} & D_{12} & B_{12}^s & D_{12}^s & H_{12}^s \\ A_{66} & D_{66} & B_{66}^s & D_{66}^s & H_{66}^s \end{Bmatrix} = \int_{\frac{-h}{2}-C}^{\frac{h}{2}-C} Q_{11}\left(1, z_{ns}^2, f(z_{ns}), z_{ns} f(z_{ns}), f^2(z_{ns})\right) \begin{Bmatrix} 1 \\ \nu \\ \frac{1-\nu}{2} \end{Bmatrix} dz_{ns} \tag{21a}$$

and

$$\left(A_{22}, D_{22}, B_{22}^s, D_{22}^s, H_{22}^s\right) = \left(A_{11}, D_{11}, B_{11}^s, D_{11}^s, H_{11}^s\right) \tag{21b}$$

$$A_{44}^s = A_{55}^s = \int_{-\frac{h}{2}-C}^{\frac{h}{2}-C} Q_{55}\left[g(z_{ns})\right]^2 dz_{ns}, \tag{21c}$$

Substituting from Eq. (19) into Eq. (18), we obtain the following equation

$$A_{11}\frac{\partial^2 u_0}{\partial x^2} + A_{66}\frac{\partial^2 u_0}{\partial y^2} + \left(A_{12} + A_{66}\right)\frac{\partial^2 v_0}{\partial x \partial y} - B_{11}^s\frac{\partial^3 w_s}{\partial x^3} - \left(B_{12}^s + 2B_{66}^s\right)\frac{\partial^3 w_s}{\partial x \partial y^2} = 0 \tag{22a}$$

$$\begin{aligned} &\left(A_{12} + A_{66}\right)\frac{\partial^2 u_0}{\partial x \partial y} + A_{66}\frac{\partial^2 v_0}{\partial x^2} + A_{22}\frac{\partial^2 v_0}{\partial y^2} - B_{22}^s\frac{\partial^3 w_s}{\partial y^3} - \left(B_{12}^s + 2B_{66}^s\right)\frac{\partial^3 w_s}{\partial x^2 \partial y} \\ &= -D_{11}\frac{\partial^4 w_b}{\partial x^4} - 2\left(D_{12} + 2D_{66}\right)\frac{\partial^4 w_b}{\partial x^2 \partial y^2} - D_{22}\frac{\partial^4 w_b}{\partial y^4} - D_{11}^s\frac{\partial^4 w_s}{\partial x^4} \\ &- 2\left(D_{12}^s + 2D_{66}^s\right)\frac{\partial^4 w_s}{\partial x^2 \partial y^2} - D_{22}^s\frac{\partial^4 w_s}{\partial y^4} = q \end{aligned} \tag{22b}$$

$$\begin{aligned} &- D_{11}\frac{\partial^4 w_b}{\partial x^4} - 2\left(D_{12} + 2D_{66}\right)\frac{\partial^4 w_b}{\partial x^2 \partial y^2} - D_{22}\frac{\partial^4 w_b}{\partial y^4} \\ &- D_{11}^s\frac{\partial^4 w_s}{\partial x^4} - 2\left(D_{12}^s + 2D_{66}^s\right)\frac{\partial^4 w_s}{\partial x^2 \partial y^2} - D_{22}^s\frac{\partial^4 w_s}{\partial y^4} = q \end{aligned} \tag{22c}$$

$$\begin{aligned} &B_{11}^s\frac{\partial^3 u_0}{\partial x^3} + \left(B_{12}^s + 2B_{66}^s\right)\frac{\partial^3 u_0}{\partial x \partial y^2} + \left(B_{12}^s + 2B_{66}^s\right)\frac{\partial^3 v_0}{\partial x^2 \partial y} + B_{22}^s\frac{\partial^3 v_0}{\partial y^3} \\ &- D_{11}^s\frac{\partial^4 w_b}{\partial x^4} - 2\left(D_{12}^s + 2D_{66}^s\right)\frac{\partial^4 w_b}{\partial x^2 \partial y^2} - D_{22}^s\frac{\partial^4 w_b}{\partial y^4} \\ &- H_{11}^s\frac{\partial^4 w_s}{\partial x^4} - 2\left(H_{12}^s + 2H_{66}^s\right)\frac{\partial^4 w_s}{\partial x^2 \partial y^2} - H_{22}^s\frac{\partial^4 w_s}{\partial y^4} + A_{55}^s\frac{\partial^2 w_s}{\partial x^2} + A_{44}^s\frac{\partial^2 w_s}{\partial y^2} = q \end{aligned} \tag{22d}$$

3. Analytical solution

Rectangular plates are generally classified in accordance with the type of support used. We are here concerned with the exact solution of Eqs. (22a)-(22d) for a simply supported FG plate. The following boundary conditions are imposed at the side edges

$$v_0 = w_b = w_s = \frac{\partial w_b}{\partial y} = \frac{\partial w_s}{\partial y} = N_x = M_x^b = M_x^s = 0 \quad \text{at} \quad x = -\frac{a}{2}, \frac{a}{2} \tag{23a}$$

$$u_0 = w_b = w_s = \frac{\partial w_b}{\partial x} = \frac{\partial w_s}{\partial x} = N_y = M_y^b = M_y^s = 0 \quad \text{at} \quad y = -\frac{b}{2}, \frac{b}{2} \tag{23b}$$

The equations of motion admit the Navier solutions for simply supported plates. The variables u_0, v_0, w_b, w_s can be written by assuming the following variations

$$\begin{Bmatrix} u_0 \\ v_0 \\ w_b \\ w_s \end{Bmatrix} = \sum_{m=1}^{\infty}\sum_{n=1}^{\infty} \begin{Bmatrix} U_{mn} \cos(\lambda x)\sin(\mu y) \\ V_{mn} \sin(\lambda x)\cos(\mu y) \\ W_{bmn} \sin(\lambda x)\sin(\mu y) \\ W_{smn} \sin(\lambda x)\sin(\mu y) \end{Bmatrix} \tag{24}$$

U_{mm}, V_{mm}, W_{bmn}, and W_{smn} are arbitrary parameters to be determined, and $\lambda = m\pi / a$ and $\mu = n\pi / b$. Further, the transverse load q is also expanded in double Fourier series as

$$q(x, y) = \sum_{m=1}^{\infty}\sum_{n=1}^{\infty} q_{mn} \sin\frac{m\pi x}{a} \sin\frac{n\pi y}{b} \tag{25}$$

For the case of a sinusoidally distributed load, we have

$$m = n = 1 \quad \text{and} \quad q_{11} = q_0 \tag{26}$$

where q_0 represents the intensity of the load at the plate centre.

Eqs. (24), (25) and Eq. (26) reduce the governing Eq. (22) to the following form

$$[C]\{\Delta\} = \{P\} \tag{27}$$

where

$$\{\Delta\}^T = \{U_{mn}, V_{mn}, W_{bmn}, W_{smn}\} \quad \text{and} \quad \{f\}^T = \{0, 0, q_{mn}, q_{mn}\}$$

where $[C]$ refers to the flexural stiffness.

4. Results and discussion

The study has been focused on the static behavior of functionally graded plate based on the present new hyperbolic shear deformation plate theory and based on neutral surface position.

For static analysis the plates are subjected to a sinusoidal distributed transverse load given by

$$q(x,y)=q_0\sin\frac{\pi x}{a}\sin\frac{\pi y}{b} \tag{28}$$

A functionally graded material consisting of Aluminum - Alumina is considered. The following material properties are used in computing the numerical values.

Ceramic (Alumina, Al_2O_3): $E_c = 380$ GPa; $\nu = 0.3$.
Metal (Aluminium, Al): $E_m = 70$ GPa; $\nu = 0.3$.

And their properties change through the thickness of the plate according to power-law. The bottom surfaces of the FG plate are aluminium rich, whereas the top surfaces of the FG plate are alumina rich.

For convenience, the following dimensionless form is used

Table 1 Effects of volume fraction exponent on the dimensionless displacements of a FGM

n	Model	$\bar{u}$	$\bar{v}$	$\bar{w}$
Ceramic	ZSDT*	0.21805	0.14493	0.29423
	HSDT#	0.21805	0.14493	0.29423
	Present	0.21815	0.144885	0.29604
0.2	ZSDT*	0.2818	0.1985	0.33672
	HSDT#	0.28172	0.19820	0.33767
	Present	0.30479	0.21538	0.35988
0.5	ZSDT*	0.42135	0.31096	0.44387
	HSDT#	0.42131	0.31034	0.44407
	Present	0.43859	0.32549	0.45369
1	ZSDT*	0.64258	0.49673	0.59059
	HSDT#	0.64137	0.49438	0.58895
	Present	0.64112	0.49408	0.58893
2	ZSDT*	0.9022	0.71613	0.76697
	HSDT#	0.89858	0.71035	0.75747
	Present	0.89793	0.70968	0.75733
5	ZSDT*	1.06786	0.84942	0.94325
	HSDT#	1.06297	0.84129	0.90951
	Present	1.06620	0.84399	0.91171
Metallic	ZSDT*	1.18373	0.78677	1.59724
	HSDT#	1.18373	0.78677	1.59724
	Present	1.18428	0.78652	1.60709

Results form Ref (Reddy 2000)
* Results from Ref (Dharan *et al*. 2010)

$$\bar{w} = 10\frac{E_C h^3}{q_0 a^4} w\left(\frac{a}{2},\frac{b}{2}\right), \qquad \bar{u} = 100\frac{E_C h^3}{q_0 a^4} u\left(0,\frac{b}{2},\frac{-h}{4}-c\right), \quad \bar{v} = 100\frac{E_C h^3}{q_0 a^4} v\left(\frac{a}{2},0,\frac{-h}{6}-c\right)$$

$$\bar{\sigma}_x = \frac{h}{hq_0}\sigma_x\left(\frac{a}{2},\frac{b}{2},\frac{h}{2}-c\right), \quad \bar{\sigma}_y = \frac{h}{hq_0}\sigma_y\left(\frac{a}{2},\frac{b}{2},\frac{h}{3}-c\right), \qquad \bar{\tau}_{xy} = \frac{h}{hq_0}\tau_{xy}\left(0,0,-\frac{h}{3}-c\right)$$

$$\bar{\tau}_{xz} = \frac{h}{hq_0}\tau_{xz}\left(0,\frac{b}{2},-c\right), \qquad \bar{\tau}_{yz} = \frac{h}{hq_0}\tau_{yz}\left(\frac{a}{2},0,\frac{h}{6}-c\right).$$

Results are tabulated in Tables 1 and 2. The tables contain the non dimensionalised deflections and stresses respectively.

The results obtained are compared with the Zeroth order Shear Deformation Theory (ZSDT) (Dharan *et al*. 2010). The present model predicts better estimates than ZSDT and is in good agreement with the most accepted model of Reddy (2000).

Table 2 Effects of volume fraction exponent on the dimensionless stresses of a FGM square plate subjected to sinusoidal loading (a / h = 10)

n	Model	$\bar{\sigma}_x$	$\bar{\sigma}_y$	$\bar{\tau}_{xy}$	$\bar{\tau}_{xz}$	$\bar{\tau}_{yz}$
Ceramic	ZSDT*	1.98915	1.31035	0.70557	0.23778	0.23778
	HSDT#	1.98915	1.31035	0.70557	0.23778	0.19051
	Present	1.99515	1.31219	0.70656	0.24406	0.21289
0.2	ZSDT*	2.1227	1.30962	0.6678	0.22557	0.2256
	HSDT#	2.12671	1.30958	0.66757	0.22532	0.18045
	Present	2.26002	1.38706	0.72053	0.24805	0.22655
0.5	ZSDT*	2.60436	1.47175	0.66709	0.23909	0.23869
	HSDT#	2.61051	1.47147	0.66668	0.23817	0.19071
	Present	2.61929	1.45863	0.69119	0.24945	0.24311
1	ZSDT*	3.07011	1.48935	0.61395	0.22705	0.23919
	HSDT#	3.08501	1.4898	0.61111	0.23817	0.19071
	Present	3.08640	1.48954	0.611061	0.24406	0.26178
2	ZSDT*	3.58089	1.3968	0.54947	0.22705	0.22719
	HSDT#	3.60664	1.39575	0.54434	0.22568	0.1807
	Present	3.60856	1.39561	0.54413	0.22427	0.27558
5	ZSDT*	4.19547	1.1087	0.57811	0.21792	0.21813
	HSDT#	4.24293	1.10539	0.57368	0.21609	0.17307
	Present	4.24758	1.10329	0.57553	0.19919	0.24164
Metallic	ZSDT*	1.98915	1.31035	0.70557	0.23778	0.23778
	HSDT#	1.98915	1.31035	0.70557	0.23778	0.19051
	Present	1.99515	1.31219	0.70656	0.24406	0.21289

The results obtained based on Reddy's HSDT (2000)

* Results from Ref (Dharan *et al*. 2010)

The table shows the effect of volume fraction exponent (V_f) on the stresses and displacements of a functionally graded square plate with $a/h = 10$. It can be observed that as the plate becomes more and more metallic the deflection $\overline{w}$ and normal stress $\overline{\sigma}_x$ increases but normal stress $\overline{\sigma}_y$ decreases. It is very interesting to note that the stresses for a fully ceramic plate are the same as that of a fully metal plate. This is due to the fact that in these two cases the plate is fully homogeneous and stresses do not depend on the Modulus of elasticity.

Fig. 4 shows the variation of non dimensionalised central deflection of a square plate with power law index n. Figs. 5 and 6 show the variation of central deflection with aspect ratio (a/b) and side to thickness ratio (a/h). It is observed that the deflection is maximum for metallic plate and minimum for a ceramic plate. The difference increases as the aspect ratio increases while it may be unchanged with the increase of side to thickness ratio.

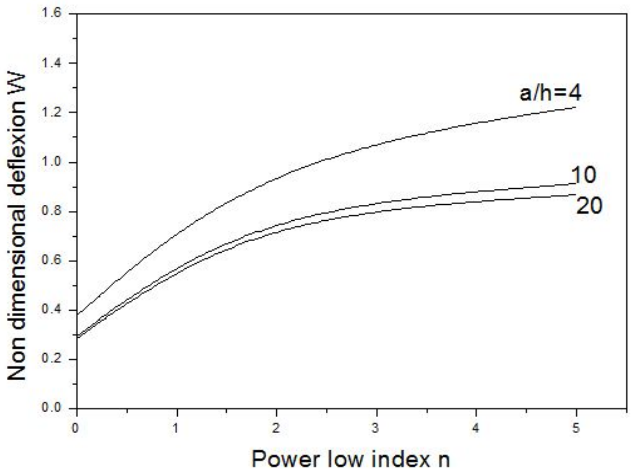

Fig. 4 Non dimensionalised central delfection $\overline{w}$ versus power law index n for a simply Supported square FGM plate under sinusoidal load

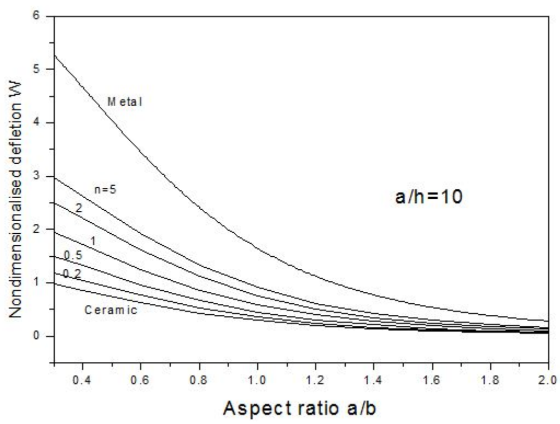

Fig. 5 Non dimensionalised central deflection $\overline{w}$ versus aspect ratio (a/b) of an FGM plate

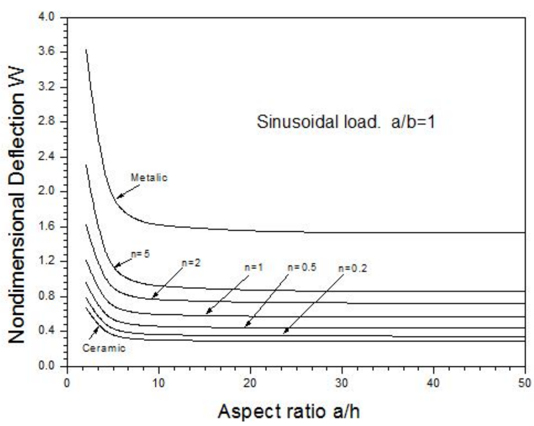

Fig. 6 Non dimesionalised central deflection $\overline{w}$ as a function of the side to thickness ratio (a/h) of an FGM square plate

From these figures it is also evident that the response of FGM plates is intermediate to that of the ceramic and metal homogeneous plates.

Figs. 7 to 11 show the distribution of normal stresses and shear stresses through the thickness of the FGM plates. The volume fraction exponent is taken as 2 for these results.

It can be seen from the Figs. 7 and 8 that the normal stresses σ_x and σ_y are compressive throughout the plate up to $\bar{z} \approx 0.149$ and then they become tensile.

Maximum values of these stresses as well as in plane shear stress τ_{xy} occur at the top and bottom surfaces of the plate.

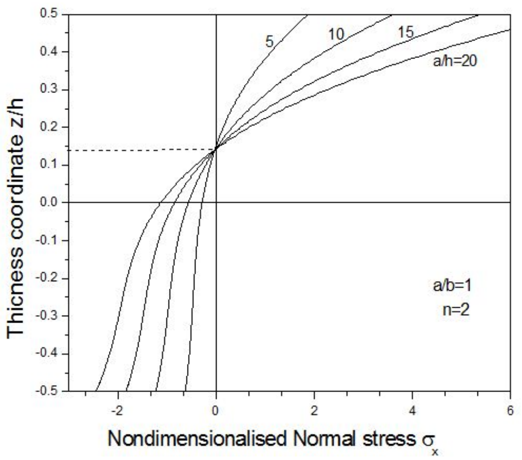

Fig. 7 Variation of In plane longitudinal stresses $\bar{\sigma}_x$ through the thickness of an FGM plate for different values of side to thickness ratio (a/h)

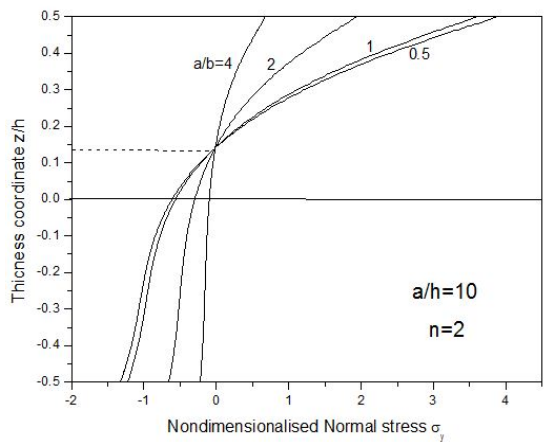

Fig. 8 Variation of In plane longitudinal stresses $\bar{\sigma}_y$ through the thickness of an FGM plate for different values of aspect ratio (a/b)

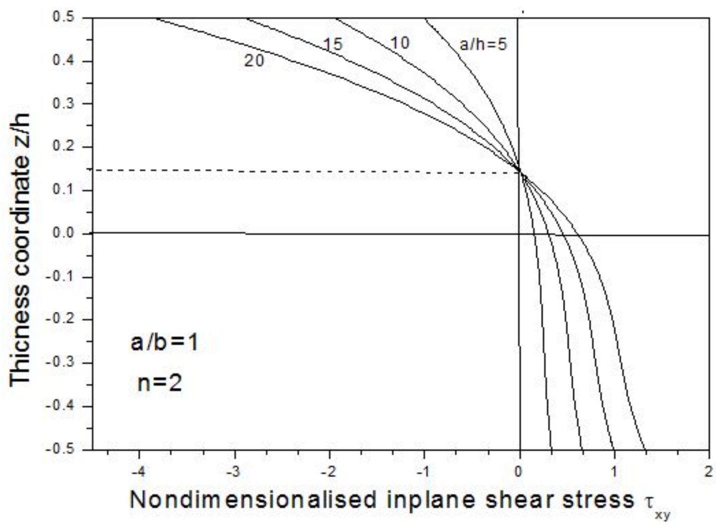

Fig. 9 Variation of In plane shear stresses $\bar{\tau}_{xy}$ through the thickness of an FGM plate for different values of side to thickness ratio (a/h)

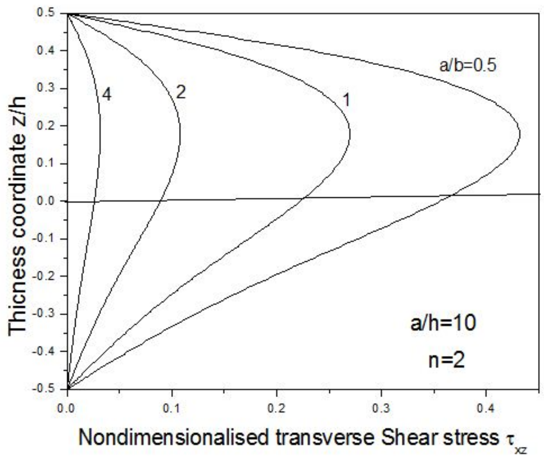

Fig. 10 Variation of transvese shear stresses $\bar{\tau}_{xz}$ through the thickness of an FGM plate for different values of aspect ratio ($a\,/\,b$)

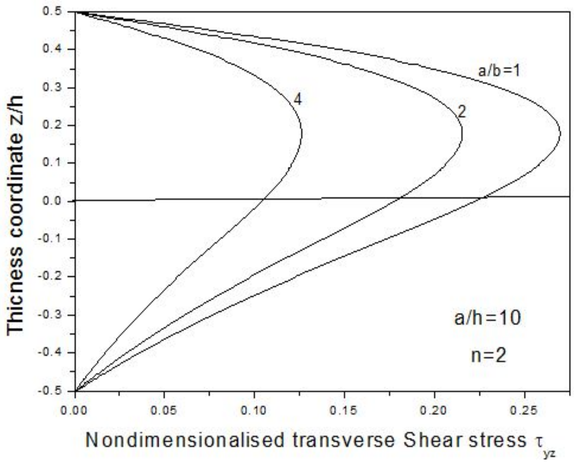

Fig. 11 Variation of transvese shear stresses $\bar{\tau}_{yz}$ through the thickness of an FGM plate for different values of aspect ratio ($a\,/\,b$)

Distinction between the curves in Figs. 10 and 11 is obvious. As strain gradients increase, the in homogeneities play a greater role in stress distribution calculations. The through-the-thickness distributions of the shear stresses τ_{yz} and τ_{xz} are not parabolic and the stresses increase as the aspect ratio decreases. It is to be noted that the maximum value occurs at $\bar{z} \approx 0.2$, not at the plate center as in the homogeneous case.

5. Conclusions

In the present study, a refined trigonometric shear deformation beam theory based on neutral surface position is proposed for free vibration analysis of functionally graded beams. The theory gives a parabolic distribution of the transverse shear strains and satisfies the zero traction boundary conditions on the surfaces of the beam without using shear correction factors. Based on the present beam theory and the neutral surface concept, the equations of motion are derived from Hamilton's principle. Numerical examples show that the proposed theory gives solutions which are almost identical with those obtained using other shear deformation theories.

References

Ait Amar Meziane, M., Abdelaziz, H.H. and Tounsi, A. (2014), "An efficient and simple refined theory for buckling and free vibration of exponentially graded sandwich plates under various boundary conditions", *J. Sandw. Struct. Mater.*, **16**(3), 293-318.

Ait Yahia, S., Ait Atmane, H., Houari, M.S.A. and Tounsi, A. (2015), "Wave propagation in functionally graded plates with porosities using various higher-order shear deformation plate theories", *Struct. Eng. Mech., Int. J.,* **53**(6), 1143-1165.

Attia, A., Tounsi, A., Adda Bedia, E.A. and Mahmoud, S.R. (2015), "Free vibration analysis of functionally graded plates with temperature-dependent properties using various four variable refined plate theories", *Steel Compos. Struct., Int. J.*, **18**(1), 187-212.

Bachir Bouiadjra, M., Houari, M.S.A. and Tounsi, A. (2012), "Thermal buckling of functionally graded plates according to a four-variable refined plate theory", *J. Therm. Stress.*, **35**(8), 677-694.

Bachir Bouiadjra, R., Adda Bedia, E.A. and Tounsi, A. (2013), "Nonlinear thermal buckling behavior of functionally graded plates using an efficient sinusoidal shear deformation theory", *Struct. Eng. Mech., Int. J.*, **48**(4), 547-567.

Belabed, Z., Houari, M.S.A., Tounsi, A., Mahmoud, S.R. and Anwar Bég, O. (2014), "An efficient and simple higher order shear and normal deformation theory for functionally graded material (FGM) plates", *Compos.: Part B*, **60**, 274-283.

Belkorissat, I., Houari, M.S.A., Tounsi, A., Adda Bedia, E.A. and Mahmoud, S.R. (2015), "On vibration properties of functionally graded nano-plate using a new nonlocal refined four variable model", *Steel Compos. Struct., Int. J.*, **18**(5). [In press]

Benachour, A., Hassaine Daouadji, T., Ait Atmane, H., Tounsi, A. and Meftah. S.A. (2011), "A four variable refined plate theory for free vibrations of functionally graded plates with arbitrary gradient", *Compos. Part B: Eng.*, **42**(6), 1386-1394.

Bessaim, A., Houari, M.S.A., Tounsi, A., Mahmoud, S.R. and Adda Bedia, E.A. (2013), "A new higher-order shear and normal deformation theory for the static and free vibration analysis of sandwich plates with functionally graded isotropic face sheets", *J. Sandw. Struct. Mater.*, **15**(6), 671-703.

Bouderba, B., Houari, M.S.A. and Tounsi, A. (2013), "Thermomechanical bending response of FGM thick plates resting on Winkler-Pasternak elastic foundations", *Steel Compos. Struct., Int. J.*, **14**(1), 85-104.

Bourada, M., Tounsi, A., Houari, M.S.A. and Adda Bedia, E.A. (2012), "A new four-variable refined plate theory for thermal buckling analysis of functionally graded sandwich plates", *J. Sandw. Struct. Mater.*, **14**(1), 5-33.

Bouremana, M., Houari, M.S.A., Tounsi, A., Kaci, A. and Adda Bedia, E.A. (2013), "A new first shear deformation beam theory based on neutral surface position for functionally graded beams", *Steel Compos. Struct., Int. J.*, **15**(5), 467-479.

Bousahla, A.A., Houari, M.S.A., Tounsi, A. and Adda Bedia, E.A. (2014), "A novel higher order shear and normal deformation theory based on neutral surface position for bending analysis of advanced composite plates", *Int. J. Comput. Method.*, **11**(6), 1350082.

Chakraverty, S. and Pradhan, K.K. (2014), "Free vibration of exponential functionally graded rectangular plates in thermal environment with general boundary conditions", *Aerosp. Sci. Technol.*, **36**, 132-156.

Dharan, S., Syam Prakash, V. and Savithri, S. (2010), "A higher order shear deformation model for functionally graded plates", *International Conference on Technological Trends* (*ICTT-2010*), Trivandrum, India, November.

Draiche, K., Tounsi, A. and Khalfi, Y. (2014), "A trigonometric four variable plate theory for free vibration of rectangular composite plates with patch mass", *Steel Compos. Struct., Int. J.*, **17**(1), 69-81.

Ebrahimi, F. (2013), "Analytical investigation on vibrations and dynamic response of functionally graded plate integrated with piezoelectric layers in thermal environment", *Mech. Adv. Mater. Struct.*, **20**(10), 854-870.

El Meiche, N., Tounsi, A., Ziane, N., Mechab, I. and Adda Bedia, E.A. (2011), "A new hyperbolic shear deformation theory for buckling and vibration of functionally graded sandwich plate", *Int. J. Mech. Sci.*, **53**(4), 237-247.

Fahsi, B., Kaci, A., Tounsi, A. and Adda Bedia, E.A. (2012), "A four variable refined plate theory for nonlinear cylindrical bending analysis of functionally graded plates under thermomechanical loadings", *J. Mech. Sci. Technol.*, **26**(12), 4073-4079.

Fekrar, A., El Meiche, N., Bessaim, A., Tounsi, A. and Adda Bedia, E.A. (2012), "Buckling analysis of functionally graded hybrid composite plates using a new four variable refined plate theory", *Steel Compos. Struct., Int. J.*, **13**(1), 91-107.

Fekrar, A., Houari, M.S.A., Tounsi, A. and Mahmoud, S.R. (2014), "A new five-unknown refined theory based on neutral surface position for bending analysis of exponential graded plates", *Meccanica*, **49**(4), 795-810.

Hadji, L., Atmane, H.A., Tounsi, A., Mechab, I. and Adda Bedia, E.A. (2011), “Free vibration of functionally graded sandwich plates using four variable refined plate theory”, *Appl. Math. Mech.*, **32**(7), 925-942.

Hamidi, A., Houari, M.S.A., Mahmoud, S.R. and Tounsi, A. (2015), “A sinusoidal plate theory with 5-unknowns and stretching effect for thermomechanical bending of functionally graded sandwich plates”, *Steel Compos. Struct., Int. J.*, **18**(1), 235-253.

Hebali, H., Tounsi, A., Houari, M.S.A., Bessaim, A. and Adda Bedia, E.A. (2014), “New quasi-3D hyperbolic shear deformation theory for the static and free vibration analysis of functionally graded plates”, *J. Eng. Mech. (ASCE)*, **140**(2), 374-383.

Houari, M.S.A., Benyoucef, S., Mechab, I., Tounsi, A., Adda Bedia, E.A. (2011), “Two variable refined plate theory for thermoelastic bending analysis of functionally graded sandwich plates”, *J. Therm. Stress.*, **34**(4), 315-334.

Houari, M.S.A., Tounsi, A., Anwar Bég, O. (2013), “Thermoelastic bending analysis of functionally graded sandwich plates using a new higher order shear and normal deformation theory”, *Int. J. Mech. Sci.*, **76**, 102-111.

Jha, D.K., Kant, T. and Singh, R.K. (2011), “Stress analysis of transversely loaded functionally graded plates with a higher order shear and normal deformation theory”, *J. Eng. Mech.*, **139**(12), 1663-1680.

Kettaf, F.Z., Houari, M.S.A., Benguediab, M. and Tounsi, A. (2013), “Thermal buckling of functionally graded sandwich plates using a new hyperbolic shear displacement model”, *Steel Compos. Struct., Int. J.*, **15**(4), 399-423.

Khalfi, Y., Houari, M.S.A. and Tounsi, A. (2014), “A refined and simple shear deformation theory for thermal buckling of solar functionally graded plates on elastic foundation”, *Int. J. Comput. Method.*, **11**(5), 1350077.

Klouche Djedid, I., Benachour, A., Houari, M.S.A., Tounsi, A. and Ameur, M. (2014), “A *n*-order four variable refined theory for bending and free vibration of functionally graded plates”, *Steel Compos. Struct., Int. J.*, **17**(1), 21-46.

Larbi Chaht, F., Kaci, A., Houari, M.S.A., Tounsi, A., Anwar Bég, O. and Mahmoud, S.R. (2014), “Bending and buckling analyses of functionally graded material (FGM) size-dependent nanoscale beams including the thickness stretching effect”, *Steel Compos. Struct., Int. J.*, **18**(2), 425-442.

Nedri, K., El Meiche, N. and Tounsi, A. (2014), “Free vibration analysis of laminated composite plates resting on elastic foundations by using a refined hyperbolic shear deformation theory”, *Mech. Compos. Mater.*, **49**(6), 641-650.

Ould Larbi, L., Kaci, A., Houari, M.S.A. and Tounsi, A. (2013), “An efficient shear deformation beam theory based on neutral surface position for bending and free vibration of functionally graded beams”, *Mech. Based Des. Struct. Machines*, **41**(4), 421-433.

Reddy, J.N. (2000), “Analysis of functionally graded plates”, *Int. J. Numer. Method. Eng.*, **47**(1-3), 663-684.

Sadoune, M., Tounsi, A., Houari, M.S.A. and Adda Bedia, E.A. (2014), “A novel first-order shear deformation theory for laminated composite plates”, *Steel Compos. Struct., Int. J.*, **17**(3), 321-338.

Saidi, H., Houari, M.S.A., Tounsi, A. and Adda Bedia, E.A. (2013), “Thermo-mechanical bending response with stretching effect of functionally graded sandwich plates using a novel shear deformation theory”, *Steel Compos. Struct., Int. J.*, **15**(2), 221-245.

Suresh, A. and Mortensen, A. (1998), *Fundamentals of Functionally Graded Materials*, Maney, London, UK.

Swaminathan, K. and Naveenkumar, D.T. (2014), “Higher order refined computational models for the stability analysis of FGM plates: Analytical solutions”, *Eur. J. Mech. A/Solids*, **47**, 349-361.

Taj, M.N.A.G., Chakrabarti, A. and Sheikh, A.H. (2013), “Analysis of functionally graded plates using higher order shear deformation theory”, *Appl. Math. Model.*, **37**(18-19), 8484-8494.

Talha, M. and Singh, B.N. (2011), “Large amplitude free flexural vibration analysis of shear deformable FGM plates using nonlinear finite element method”, *Finite Elem. Anal. Des.*, **47**(4), 394-401.

Tounsi, A., Houari, M.S.A., Benyoucef, S. and Adda Bedia, E.A. (2013), “A refined trigonometric shear deformation theory for thermoelastic bending of functionally graded sandwich plates”, *Aerosp. Sci.*

Technol., **24**(1), 209-220.
Zidi, M., Tounsi, A., Houari, M.S.A., Adda Bedia, E.A. and Anwar Bég, O. (2014), "Bending analysis of FGM plates under hygro-thermo-mechanical loading using a four variable refined plate theory", *Aerosp*. *Sci*. *Technol*., **34**, 24-34.

CC